

Quark spin - thermal vorticity alignment and the Λ , $\bar{\Lambda}$ polarization in heavy-ion collisions

Alejandro Ayala^{1,2}, D. de la Cruz^{1,3}, L. A. Hernández^{1,2,4},
S. Hernández-Ortíz⁵ and J. Salinas¹

¹ Instituto de Ciencias Nucleares, Universidad Nacional Autónoma de México, Apartado Postal 70-543, México, Distrito Federal 04510, Mexico

² Centre for Theoretical and Mathematical Physics, and Department of Physics, University of Cape Town, Rondebosch 7700, South Africa

³ Departamento de Física, Escuela Superior de Física y Matemáticas del Instituto Politécnico Nacional, Unidad Adolfo López Mateos, Edificio 9, 07738 Ciudad de México, México

⁴ Facultad de Ciencias de la Educación, Universidad Autónoma de Tlaxcala, Tlaxcala, 90000, Mexico

⁵ Institute of Nuclear Theory, University of Washington, Physics-Astronomy Building, Seattle 98195-1550, United States of America

E-mail: ayala@nucleares.unam.mx

Abstract. It has been proposed that the Λ and $\bar{\Lambda}$ polarizations observed in heavy-ion collisions are due to the interaction between quark spin and thermal vorticity. In this work we report on a computation of the relaxation time required for this alignment to occur at finite temperature and baryon chemical potential, considering quarks with a finite mass. The calculation is performed after modelling the interaction by means of an effective vertex which couples the thermal gluons and quarks within the vortical medium. We show that the effect of the quark mass is to reduce the relaxation time as compared to the massless quark case. An intrinsic global polarization of quarks/antiquarks emerges which is shown to be linked with the $\Lambda/\bar{\Lambda}$ polarization.

1. Introduction

Experiments where heavy-ions collide at relativistic energies provide a unique opportunity to investigate the properties of hadronic matter under extreme conditions of temperature and density, conditions that are analogous to those found soon after the Big Bang. At experimental facilities such as RHIC and the LHC and in coming years at J-PARC, FAIR, and NICA two atomic nuclei collide at relativistic energies giving rise to sequential stages of strongly interacting matter dynamics, among these, the quark-gluon plasma (QGP) phase. It has been suggested that during the QGP stage a kinematic vorticity of the order of $\omega \sim 10^{22} \text{ s}^{-1}$ can be achieved in collisions at RHIC

and LHC energies, thus establishing QGP as the most vortical fluid known so far [1]. The vorticity is capable to transfer angular momentum to the spin degrees of freedom of primary quarks, originating the so-called global baryon polarization once polarized quarks hadronize [2]. Since QGP can be very well described using hydrodynamical models, a relativistic hydro description of the classical vorticity led to the concept of thermal vorticity [3, 4] defined as

$$\bar{\omega}_{\mu\nu} = \frac{1}{2} (\partial_\nu \beta_\mu - \partial_\mu \beta_\nu), \quad (1)$$

where $\beta_\mu = u_\mu(x)/T(x)$, $u_\mu(x)$ is the local fluid four-velocity and $T(x)$ is the local temperature. Thermal vorticity describes a rotating fluid that is able to generate a global particle polarization. An outstanding question is what is the time for the spin degrees of freedom to equilibrate with the thermal vorticity. The question is similar to that of finding the time for the momentum degrees of freedom to equilibrate and achieve a common temperature.

2. Quark Spin - Thermal Vorticity Alignment

Current hydrodynamical descriptions indicate that the QCD plasma reaches a state of local thermal equilibrium within $\tau_{\text{hydro}} \sim 1$ fm [5]. After this time, the system can be approximately identified as having a temperature T and quark chemical potential μ_q . The interaction rate Γ of a quark with four-momentum $P = (p_0, \vec{p})$ can be expressed in terms of the quark self energy Σ as

$$\Gamma(p_0) = \tilde{f}(p_0 - \mu_q) \text{Tr} \{ \gamma^0 \text{Im} \Sigma \}, \quad (2)$$

where $\tilde{f}(p_0 - \mu_q)$ is the Fermi-Dirac distribution. The interaction between the thermal vorticity and the quark spin is modeled by means of a phenomenological effective vertex

$$\lambda_a^\mu = g \frac{\sigma^{\alpha\beta}}{2} \bar{\omega}_{\alpha\beta} \gamma^\mu t_a, \quad (3)$$

where $\sigma^{\alpha\beta} = \frac{i}{2} [\gamma^\alpha, \gamma^\beta]$ is the quark spin operator and t_a are the color matrices in the fundamental representation. The one-loop contribution to Σ , depicted in Fig. 1, is given explicitly by

$$\Sigma = T \sum_n \int \frac{d^3k}{(2\pi)^3} \lambda_a^\mu S(\not{P} - \not{K}) \lambda_b^{\nu*} G_{\mu\nu}^{ab}(K), \quad (4)$$

where S and $*G$ are the quark and effective gluon propagators, respectively. In a covariant gauge, the Hard Thermal Loop (HTL) approximation to the effective gluon propagator is given by

$$*G_{\mu\nu}(K) = *\Delta_L(K) P_{L\mu\nu} + *\Delta_T(K) P_{T\mu\nu}, \quad (5)$$

where $P_{L,T\mu\nu}$ are the polarization tensors for three dimensional longitudinal and transverse gluons. The gluon propagator functions for longitudinal and transverse

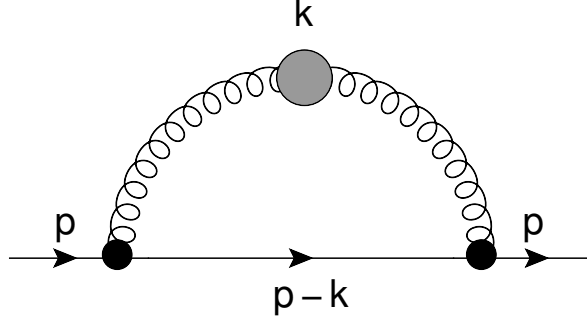


Figure 1. One-loop Feynman diagram representing the quark self-energy. The gluon line with a blob represents the effective gluon propagator at finite density and temperature. The blobs on the quark-gluon vertices represent the effective coupling between the quark spin and the vorticity.

modes, ${}^* \Delta_{L,T}(K)$, are given by

$$\begin{aligned} {}^* \Delta_L(K)^{-1} &= K^2 + 2m^2 \frac{K^2}{k^2} \left[1 - \left(\frac{i\omega_n}{k} \right) Q_0 \left(\frac{i\omega_n}{k} \right) \right], \\ {}^* \Delta_T(K)^{-1} &= -K^2 - m^2 \left(\frac{i\omega_n}{k} \right) \left\{ \left[1 - \left(\frac{i\omega_n}{k} \right)^2 \right] Q_0 \left(\frac{i\omega_n}{k} \right) + \left(\frac{i\omega_n}{k} \right) \right\}, \end{aligned} \quad (6)$$

where

$$Q_0(x) = \frac{1}{2} \ln \frac{x+1}{x-1}, \quad (7)$$

and m is the gluon thermal mass given by

$$m^2 = \frac{1}{6} g^2 C_A T^2 + \frac{1}{12} g^2 C_F \left(T^2 + \frac{3}{\pi^2} \mu^2 \right), \quad (8)$$

where $C_A = 3$ and $C_F = 4/3$ are the Casimir factors for the adjoint and the fundamental representations of $SU(3)$, respectively. The sum over Matsubara frequencies involves products of the propagator functions for longitudinal and transverse gluons ${}^* \Delta_{L,T}$ and the Matsubara propagator for the bare quark $\tilde{\Delta}_F$. Then, the sum over Matsubara frequencies can be expressed as

$$S_{L,T} = T \sum_n {}^* \Delta_{L,T}(i\omega_n) \tilde{\Delta}_F(i(\omega_m - \omega_n)), \quad (9)$$

which is evaluated introducing the spectral densities $\rho_{L,T}$ and $\tilde{\rho}$ for the gluon and fermion propagators, respectively. The imaginary part of S_i (with $i = L, T$) can thus be written as

$$\text{Im } S_i = \pi \left(e^{(p_0 - \mu_q)/T} + 1 \right) \int_{-\infty}^{\infty} \frac{dk_0}{2\pi} \int_{-\infty}^{\infty} \frac{dp'_0}{2\pi} f(k_0) \tilde{f}(p'_0 - \mu) \delta(p_0 - k_0 - p'_0) \rho_i(k_0) \tilde{\rho}(p'_0), \quad (10)$$

where $f(k_0)$ is the Bose-Einstein distribution. The spectral densities $\rho_{L,T}(k_0, k)$ are obtained from the imaginary part of ${}^*\Delta_{L,T}(i\omega_n, k)$ after the analytic continuation $i\omega_n \rightarrow k_0 + i\epsilon$ and contain the discontinuities of the gluon propagator across the real k_0 -axis. Their support depends on the ratio $x = k_0/k$. For $|x| > 1$, $\rho_{L,T}$ have support on the (time-like) quasiparticle poles. For $|x| < 1$ their support coincides with the branch cut of $Q_0(x)$. On the other hand, the spectral density corresponding to a bare quark is given by

$$\tilde{\rho}(p'_0) = 2\pi\epsilon(p'_0)\delta(p_0'^2 - E_p^2), \quad (11)$$

where $E_p^2 = (p - k)^2 + m_q^2$ with m_q the quark mass. The kinematical restriction that Eq. (11) imposes on Eq. (10) limits the integration over gluon energies to the space-like region, namely, $|x| < 1$. Therefore, the parts of the gluon spectral densities that contribute to the interaction rate are given by

$$\begin{aligned} \rho_L(k_0, k) &= \frac{x}{1-x^2} \frac{2\pi m^2 \theta(k^2 - k_0^2)}{\left[k^2 + 2m^2 \left(1 - \frac{x}{2} \ln \left| \frac{1+x}{1-x} \right| \right)^2 + [\pi m^2 x]^2 \right]}, \\ \rho_T(k_0, k) &= \frac{\pi m^2 x (1-x^2) \theta(k^2 - k_0^2)}{\left\{ k^2 (1-x^2) + m^2 \left[x^2 + \frac{x}{2} (1-x^2) \ln \left| \frac{1+x}{1-x} \right| \right] \right\}^2 + \left[\frac{\pi m^2 x (1-x^2)}{2} \right]^2}. \end{aligned} \quad (12)$$

Collecting all the ingredients, the interaction rate for a massive quark with energy p_0 to align its spin with the thermal vorticity is given by

$$\begin{aligned} \Gamma(p_0) &= \frac{\alpha_s}{4\pi} \left(\frac{\omega}{T} \right)^2 \frac{C_F}{\sqrt{p_0^2 - m_q^2}} \int_0^\infty dk k \\ &\times \int_{\mathcal{R}} dk_0 [1 + f(k_0)] \tilde{f}(p_0 + k_0 - \mu_q) \sum_{i=L,T} C_i(p_0, k_0, k) \rho_i(k_0, k), \end{aligned} \quad (13)$$

where \mathcal{R} represents the region

$$\sqrt{\left(\sqrt{p_0^2 - m_q^2} - k \right)^2 + m_q^2} - p_0 \leq k_0 \leq \sqrt{\left(\sqrt{p_0^2 - m_q^2} + k \right)^2 + m_q^2} - p_0. \quad (14)$$

The polarization coefficients $C_{L,T}$ come from the contraction of the polarization tensors $P_{L,T\mu\nu}$ with the trace of the factors involving Dirac gamma matrices from the self-energy. After implementing the kinematical restrictions for the allowed values of the angle between the quark and gluon momenta, these functions are found to be

$$\begin{aligned} C_T(p_0, k_0, k) &= 8(p_0 + k_0) \left(\frac{k^2 - 2k_0 p_0 - k_0^2}{2k \sqrt{p_0^2 - m_q^2}} \right)^2, \\ C_L(p_0, k_0, k) &= -8(p_0 + k_0) \left[\left(\frac{k^2 - 2k_0 p_0 - k_0^2}{2k \sqrt{p_0^2 - m_q^2}} \right)^2 - \frac{1}{2} \right] - 8 \frac{p_0 k^2}{k_0^2 - k^2} \left(\frac{k^2 - 2k_0 p_0 - k_0^2}{2k \sqrt{p_0^2 - m_q^2}} \right)^2. \end{aligned} \quad (15)$$

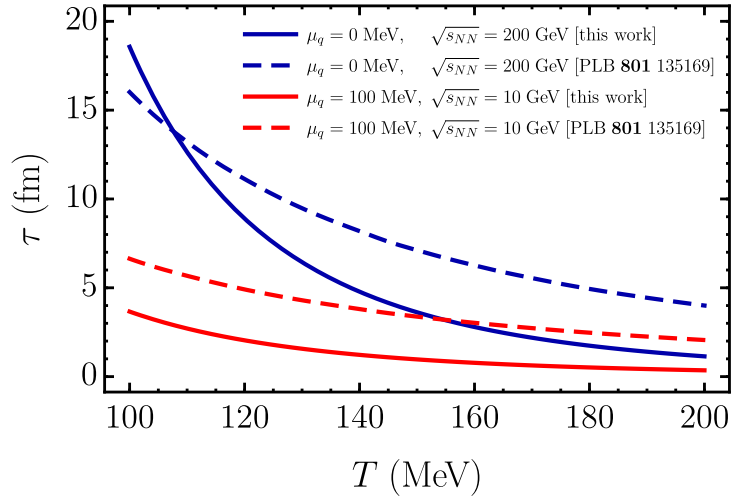


Figure 2. Relaxation time τ for quarks as a function of temperature T for semicentral collisions at an impact parameter $b = 10$ fm. In dashed lines, massless quarks [6] for $\sqrt{s_{NN}} = 10, 200$ GeV with $\omega \simeq 0.12, 0.10$ fm $^{-1}$, respectively. In solid lines, massive quarks for $\sqrt{s_{NN}} = 10, 200$ GeV with $\omega \simeq 0.072, 0.051$ fm $^{-1}$, respectively, using the findings of Ref. [7].

This result should be contrasted with Eqs. (14) of Ref. [6], *i.e.*,

$$\begin{aligned}
 C_T(p_0, k_0, k) &= 8k_0 \left(\frac{k^2 - 2k_0 p_0 - k_0^2}{2k p_0} \right)^2, \\
 C_L(p_0, k_0, k) &= -8k_0 \left[\left(\frac{k^2 - 2k_0 p_0 - k_0^2}{2k p_0} \right)^2 - \frac{1}{2} \right],
 \end{aligned} \tag{16}$$

which were computed for the $m_q \rightarrow 0$ and small quark momentum limit. The total interaction rate is obtained by integrating Eq. (13) over the available phase space

$$\Gamma = V \int \frac{d^3 p}{(2\pi)^3} \Gamma(p_0), \tag{17}$$

where V is the volume of the overlap region in the collision. Notice that, although the available phase space for a massive quark is reduced as compared to the massless quark case, the contribution of the new terms in Eqs. (15) enhance the overall interaction rate. Recall that for the collision of symmetric systems of nuclei with radii R and a given impact parameter b , V is given by

$$V = \frac{\pi}{3} (4R + b)(R - b/2)^2. \tag{18}$$

From the expression for Γ in Eq. (17), we study the parametric dependence of the relaxation time for spin and vorticity alignment, defined as

$$\tau \equiv 1/\Gamma. \tag{19}$$

3. Results

To estimate the angular velocity ω produced in semicentral collisions, we follow the findings of Ref. [7] that provide these values for given energies and impact parameters. Although ω evolves with time, we work out the computation using its initial value at full nuclei overlap. For an impact parameter $b = 10$ fm, the angular velocity was found to be $\omega \simeq 0.06, 0.04 \text{ fm}^{-1}$ for collision energies $\sqrt{s_{NN}} = 10, 200$ GeV, respectively.

The relaxation times for quarks of mass $m_q = 100$ MeV and quark chemical potential μ_q as a function of temperature are shown in Fig. 2 for two different energies. Notice that $\tau \lesssim 5$ fm for the temperature range $150 \text{ MeV} < T < 200 \text{ MeV}$, where the phase transition is expected. In this temperature range, the relaxation times are smaller than the ones found in Ref. [6] for most of the energy range considered. Notice that a finite quark mass produces a smaller relaxation time compared to the findings of Ref. [6].

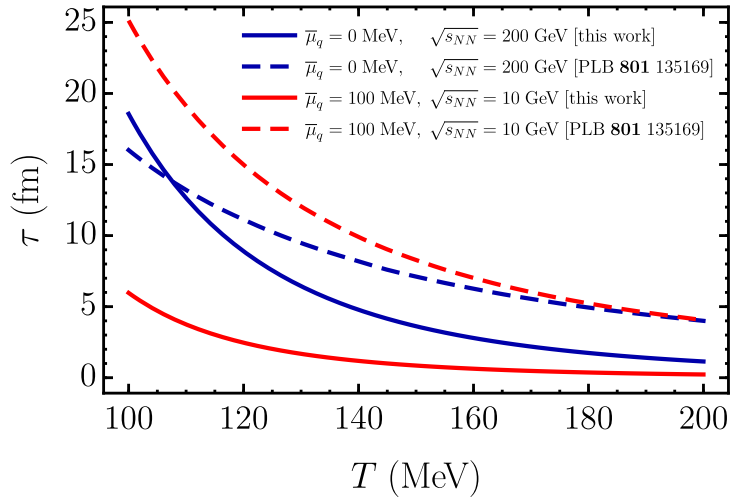


Figure 3. Relaxation time $\bar{\tau}$ for antiquarks as a function of temperature T for semicentral collisions at an impact parameter $b = 10$ fm. In dashed lines, massless quarks [6] for $\sqrt{s_{NN}} = 10, 200$ GeV with $\omega \simeq 0.12, 0.10 \text{ fm}^{-1}$, respectively. In solid lines, massive quarks for $\sqrt{s_{NN}} = 10, 200$ GeV with $\omega \simeq 0.072, 0.051 \text{ fm}^{-1}$, respectively, using the findings of Ref. [7].

For antiquarks with chemical potential $\bar{\mu}_q = -\mu_q$, the resulting relaxation times for $\sqrt{s_{NN}} = 10, 200$ GeV and an impact parameter of $b = 10$ fm are shown in Fig. 3. In order to obtain the quark/antiquark relaxation times as a function of collision energy, we use the freeze-out parametrization of Ref. [8]

$$\begin{aligned} T(\mu_B) &= 166 - 139\mu_B^2 - 53\mu_B^4, \\ \mu_B(\sqrt{s_{NN}}) &= \frac{1308}{1000 + 0.273\sqrt{s_{NN}}}, \end{aligned} \quad (20)$$

where the freeze-out baryon chemical potential μ_B and temperature T are given in MeV. These relaxation times are shown in Fig. 4 Notice that the relaxation times for

quarks show a monotonic growth as a function of the collision energy. In contrast, the corresponding relaxation times for antiquarks have a minimum for collision energies in the range $40 \text{ GeV} \lesssim \sqrt{s_{NN}} \lesssim 70 \text{ GeV}$.

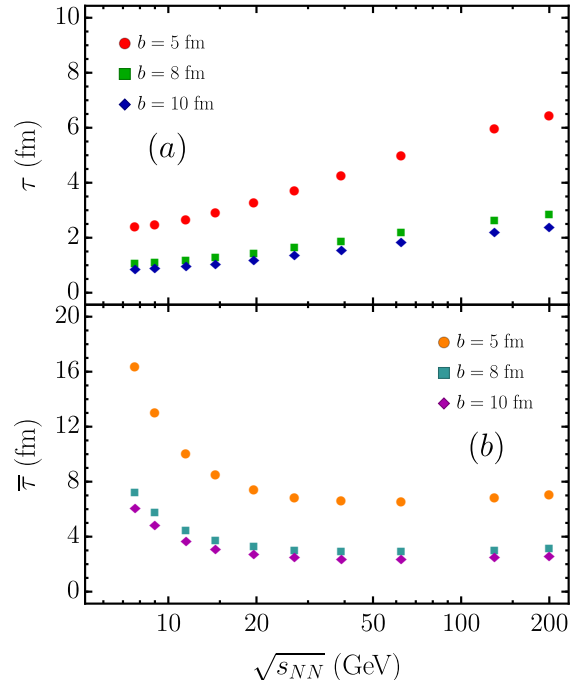


Figure 4. (a) Relaxation time τ for quarks as a function of $\sqrt{s_{NN}}$ for semicentral collisions at impact parameters $b = 5, 8, 10$ fm. (b) Relaxation time $\bar{\tau}$ for antiquarks as a function of $\sqrt{s_{NN}}$ for semicentral collisions at impact parameters $b = 5, 8, 10$ fm.

Finally, we compute the fraction of globally polarized particles as a function of time, which is given as

$$\begin{aligned}
 z &\equiv \frac{N}{N_0} = 1 - e^{-t/\tau}, \\
 \bar{z} &\equiv \frac{\bar{N}}{\bar{N}_0} = 1 - e^{-t/\bar{\tau}},
 \end{aligned}
 \tag{21}$$

where z and \bar{z} are properly referred to as the *intrinsic* global polarization for quarks and antiquarks, respectively. Notice that $\bar{z} < z$ when the impact parameter and the collision energy are the same for both quarks and antiquarks, as can be seen from Fig. 5. Both intrinsic polarizations tend to 1 for $t \simeq 10$ fm. However, a finite intrinsic global polarization for quarks and antiquarks can still be expected when the QGP phase lasts for less than 10 fm.

In conclusion, we have performed a microscopic study to estimate relaxation times for the alignment between strange quark spin and thermal vorticity at finite temperature

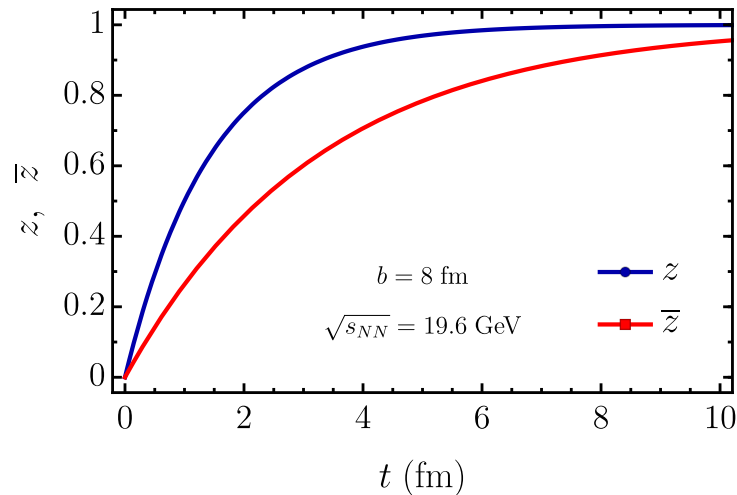


Figure 5. Intrinsic global polarization for quarks (z) and antiquarks (\bar{z}) as functions of time t for semicentral collisions at an impact parameter $b = 8$ fm for $\sqrt{s_{NN}} = 19.6$ GeV.

and baryon chemical potential, considering the effects of the quark mass in the alignment. When T and μ_B are increased and the initial angular velocity is fixed, relaxation times lie well within the expected life-time of the system, although this does not change the fact that relaxation times for antiquarks are larger than the corresponding relaxation times for quarks. It is interesting to note that during hadronization, further effects can enhance $\bar{\Lambda}$ polarization so as to obtain $\mathcal{P}_{\bar{\Lambda}} > \mathcal{P}_{\Lambda}$. For example, as discussed in this same proceedings [9] and in more detail in Ref. [10], this can happen when the reaction zone is modelled as composed of a high-density core and a less dense corona. The idea was put forward some time ago in Ref. [11]. Although both regions are subject to the vortical motion, Λ s and $\bar{\Lambda}$ s coming from one or the other regions could show different polarization properties. This can happen since their origins are different: in the core these hyperons come mainly from QGP induced processes. In the corona they come from nucleon-nucleon interaction processes. When this is considered together with a larger abundance of Λ s as compared to $\bar{\Lambda}$ s in the corona and a smaller number of Λ s coming from the core as compared to those coming from the corona, an amplification effect for the $\bar{\Lambda}$ polarization can occur. This is more prominent for semi-central to peripheral collisions and small collision energies. Further details are provided in Refs. [9, 10].

Acknowledgments

Support for this work has been received in part by UNAM-DGAPA-PAPIIT grant number IG100219 and by Consejo Nacional de Ciencia y Tecnología grant numbers A1-S-7655 and A1S16215.

References

- [1] Adamczyk L *et al.* (STAR Collaboration) 2017 *Nature* **548** 62.

- [2] Liang Z-T and Wang X-N 2005 *Phys. Lett. B* **629** 20.
- [3] Csernai L P, Magas V K and Wang D J 2013 *Phys. Rev. C* **87** 034906.
- [4] Becattini F, Chandra V, Del Zanna L and Grossi E 2013 *Ann. Phys.* **338** 32.
- [5] Liu J, Shen C and Heinz U 2015 *Phys. Rev. C* **91** 064906.
- [6] Ayala A, de la Cruz D, Hernandez-Ortiz S, Hernandez L A and Salinas J 2020 *Phys. Lett. B* **801** 135169.
- [7] Deng X-G, Huang X-G, Ma Y-G and Zhang S 2020 Vorticity in low-energy heavy-ion collisions *Preprint* nucl-th/2001.01371.
- [8] Cleymans J, Oeschler H, Redlich K and Wheaton S 2006 *Phys. Rev. C* **73** 034905.
- [9] Maldonado I 2020 Two-component source to explain Λ and $\bar{\Lambda}$ global polarization in non-central heavy-ion collisions, 36th Winter Workshop on Nuclear Dynamics, Puerto Vallarta, Mexico.
- [10] Ayala A *et al.* 2020 Core meets corona: a two-component source to explain Λ and $\bar{\Lambda}$ global polarization in semi-central heavy-ion collisions *Preprint* hep-ph/2003.13757.
- [11] Ayala A, Cuautle E, Herrera G and Montaño L M 2002 *Phys. Rev. C* **85** 024902.